Lecture Notes on
Nonlinear Inversion and Tomography:
I. Borehole Seismic Tomography

From a Series of Lectures by

James G. Berryman
University of California
Lawrence Livermore National Laboratory
Livermore, CA 94550

Originally Presented at

Earth Resources Laboratory
Massachusetts Institute of Technology

July 9–30, 1990

Revised and Expanded

October, 1991

Chapter 5

Fast Ray Tracing Methods

The most expensive step in any traveltime inversion or tomography algorithm is the forward modeling step associated with ray tracing through the current best estimate of the wave speed model. It is therefore essential to make a good choice of ray tracing algorithm for the particular application under consideration. Prior to choosing a ray tracing method, a method of representing the model must be chosen. Three typical choices are: cells or blocks of constant slowness, a rectangular grid with slowness values assigned to the grid points and linearly interpolated values between grid points, or a sum over a set of basis functions whose coefficients then determine the model. The ray tracing method should be designed to produce optimum results for the particular model representation chosen.

We will consider three approaches to ray tracing:

1. Shooting methods.
2. Bending methods.
3. Full wave equation methods.

These three methods are based respectively on Snell's law [Born and Wolf, 1980], Fermat's principle [Fermat, 1891], and Huygen's principle [Huygens, 1690]. We will find that shooting methods and wave equation methods should generally be used with smooth representations of the model such as linearly interpolated grids or spline function approximations, while bending methods are preferred for constant cell representations.

We will study each of these approaches in some detail in this section. But first we address a question commonly asked about the necessity of using bent rays in traveltime tomography.

5.1 Why Not Straight Rays?

Straight rays are used in x-ray tomography and the results obtained are very good, so why not use straight rays in seismic inversion and tomography? For x-rays traveling through the body, the index of refraction is essentially constant, so the ray paths are in fact nearly straight. Furthermore, the reconstruction in x-ray tomography is performed on the attenuation coefficient, not the wave speed, so the situation is not really comparable to that of

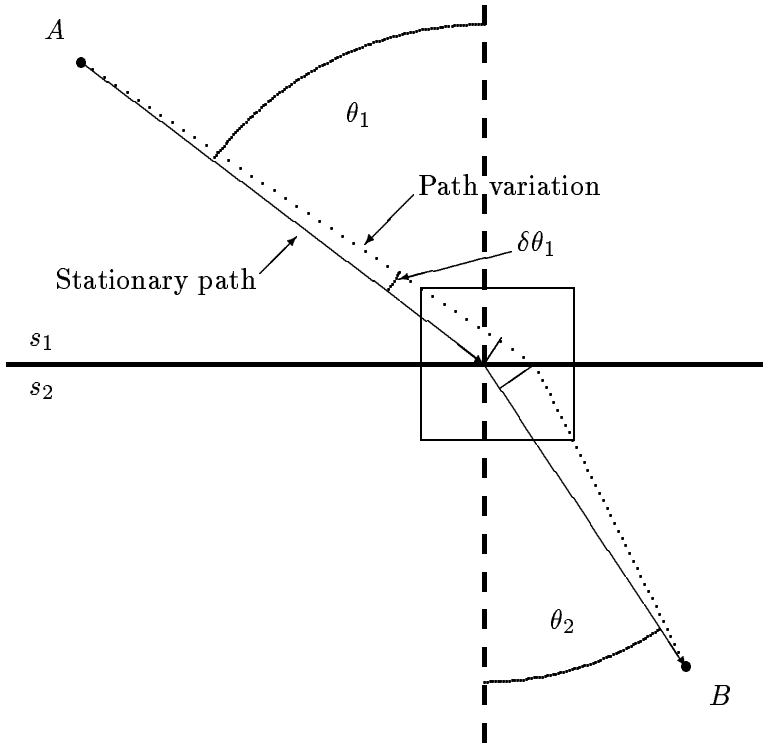

Figure 5.1: Snell's law is a consequence of the stationarity of the traveltime functional.

seismic tomography. Reconstructions in seismic inversion and tomography are most often performed on the wave speed or wave slowness. Since the earth is not homogeneous, the speed of sound varies significantly and the effective index of refraction is far from being constant. Thus, the rays in a seismic transmission experiment really do bend significantly and this fact should be taken into account in the reconstruction.

Suppose that we use straight rays in a tomographic reconstruction when in truth the rays whose traveltimes have been measured were actually bent according to Fermat's principle or Snell's law. In a region where the wave speed is quite low, the true rays will tend to go around the region, but the straight rays go through anyway. So the backprojection along a straight ray will naturally focus the effects of a slow region into a *smaller region* than it should. Similarly, in a region where the wave speed is quite high, the true rays will tend to accumulate in the fast region, whereas the straight rays are free to ignore this focusing effect. Thus, the backprojection along a straight ray will tend to defocus the effects of a fast region into a *larger region* than it should. If we could train our eyes to look for these effects in straight ray reconstructions, then it might not be essential to use bent rays. But until then, it is important to recognize that using straight rays has important effects on the resolution of the reconstruction. Regions of high wave speed will appear larger than true, so such regions are poorly resolved. Regions of low wave speed will appear smaller than

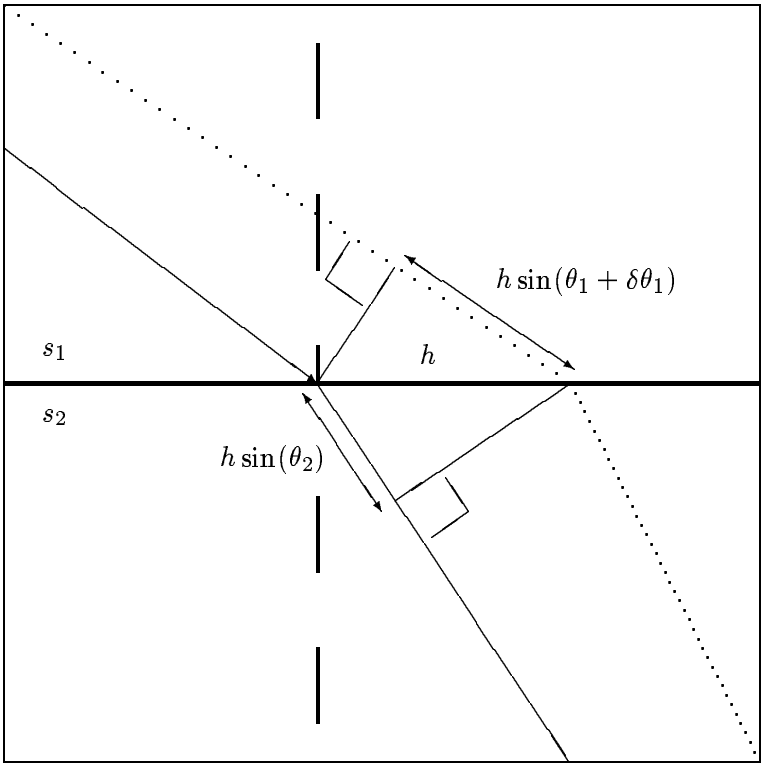

Figure 5.2: Detail of the stationarity calculation (see preceding Figure).

true, so such regions are poorly defined.

Having said all this, nevertheless there are circumstances where I would recommend using straight rays in the reconstruction. First, if the region to be imaged contains very high contrasts so that some of the assumptions normally made to speed up the ray tracing codes are expected to be violated (*e.g.*, rays double back on themselves), then stable reconstructions with bent rays may be impossible while a straight ray reconstruction can still give some useful information. Second, if the desired result is just a low resolution image showing whether or not an anomaly is present, then straight rays are entirely appropriate. Third, if a reconstruction for anisotropic wave speed is being attempted, then straight rays are recommended too, since the nonuniqueness expected in the reconstruction when bent rays are coupled with anisotropy in the model appears so overwhelming that I think little can be done to overcome the problem at the present time.[1]

Straight rays are always computed quickly since they depend only on the source and receiver locations. So if resolution is not an issue but speed of computation is, then of course straight rays can and probably should be used. However, using straight rays is limiting the reconstruction to be merely *linear inversion or tomography*, but — since our subject is *nonlinear inversion and tomography* — we will not consider straight rays further.

[1] See Jech and Pšenčík [1989; 1991].

5.2 Variational Derivation of Snell's law

For piece-wise constant slowness models, we consider Snell's law.

A medium with two regions of constant slowness s_1, s_2 is separated by a plane boundary. The ray path connecting two points, A and B, located on either side of the boundary is stationary, *i.e.*, small deviations from this path make only second order corrections to the traveltime. Referring to Figures 5.1 and 5.2, we let the solid line denote the ray path having stationary traveltime and let the dotted line be a perturbed ray path. Each path is assumed to comprise straight lines within each medium which then bend into a new direction upon crossing the boundary. We let θ_1 and θ_2 denote the angles of the stationary path from the normal to the boundary in the two regions, respectively. A simple geometrical argument can be used to infer the difference in length between the two paths to first order in h, the distance between the points where the paths intersect the boundary. We find that the segment of the perturbed path in region 1 is $h\sin(\theta_1 + \delta\theta)$ units longer than the stationary path, while in region 2 the perturbed path is $h\sin\theta_2$ units shorter. Therefore, the traveltime along the perturbed ray differs from that along the stationary ray by Δt, given by

$$\Delta t = s_1 h \sin\theta_1 - s_2 h \sin\theta_2, \tag{5.1}$$

neglecting the second order effects due to finite $\delta\theta$ and due to the slight differences in the remainders of these two paths. Since the traveltime is stationary, we set $\Delta t = 0$ and find that

$$\boxed{s_1 \sin\theta_1 \quad = \quad s_2 \sin\theta_2. \qquad \text{(Snell's law)}} \tag{5.2}$$

5.3 Ray Equations and Shooting Methods

Let the ray path P between two points A and B be represented by a trajectory $\mathbf{x}(u)$, where u is a scalar parameter that increases monotonically along the ray. We can then write the traveltime along the path as

$$t = \int_P s(\mathbf{x}(u))\, dl(u) \tag{5.3}$$

$$= \int_{u(A)}^{u(B)} f(\mathbf{x}, \dot{\mathbf{x}})\, du, \tag{5.4}$$

where $\dot{\mathbf{x}} = d\mathbf{x}/du$ and

$$f(\mathbf{x}, \dot{\mathbf{x}}) = s(\mathbf{x})|\dot{\mathbf{x}}|. \tag{5.5}$$

Fermat's principle implies that the stationary variation [Whitham, 1974]

$$\delta t = \int_{u(A)}^{u(B)} [\nabla_{\mathbf{x}} f \cdot \delta\mathbf{x} + \nabla_{\dot{\mathbf{x}}} f \cdot \delta\dot{\mathbf{x}}]\, du = 0. \tag{5.6}$$

Integrating by parts

$$\delta t = \int_{u(A)}^{u(B)} \left[\nabla_{\mathbf{x}} f - \frac{d}{du}\nabla_{\dot{\mathbf{x}}} f\right] \cdot \delta\mathbf{x} du = 0. \tag{5.7}$$

Since this must be true for all $\delta\mathbf{x}$, we can infer

$$\nabla_{\mathbf{x}} f - \frac{d}{du}\nabla_{\dot{\mathbf{x}}} f = 0. \tag{5.8}$$

Now observe that

$$\nabla_{\mathbf{x}} f = |\dot{\mathbf{x}}|\nabla s, \tag{5.9}$$

$$\nabla_{\dot{\mathbf{x}}} f = s(\mathbf{x})\frac{\dot{\mathbf{x}}}{|\dot{\mathbf{x}}|}. \tag{5.10}$$

Further, we have $dl = |\dot{\mathbf{x}}|du$, so stationarity of t implies

$$\boxed{\nabla s = \frac{d}{dl}\left(s\frac{d}{dl}\mathbf{x}\right).} \tag{5.11}$$

This is the *ray equation.*

In a 2-D application, the ray equation may be rewritten in terms of the angle θ of the ray from the x direction. First, note that

$$\frac{d}{dl}\mathbf{x} = \hat{\rho} = \cos\theta\hat{\mathbf{x}} + \sin\theta\hat{\mathbf{y}} \tag{5.12}$$

and

$$\frac{d}{dl}\hat{\rho} = \hat{\theta}\frac{d\theta}{dl} = (-\sin\theta\hat{\mathbf{x}} + \cos\theta\hat{\mathbf{y}})\frac{d\theta}{dl}, \tag{5.13}$$

so that (5.11) may be rewritten as

$$\nabla s = \frac{ds}{dl}\hat{\rho} + s\hat{\theta}\frac{d\theta}{dl}, \tag{5.14}$$

which implies

$$\hat{\theta}\cdot\nabla s = s\frac{d\theta}{dl}. \tag{5.15}$$

Finally, we obtain

$$\boxed{\frac{d\theta}{dl} = \frac{1}{s}\left(\frac{\partial s}{\partial y}\cos\theta - \frac{\partial s}{\partial x}\sin\theta\right),} \tag{5.16}$$

giving an explicit differential equation for the ray angle θ along a 2-D path.

The ray equations form the basis for shooting methods of ray tracing. Starting at any source point, we initially choose a set of possible angles. An optimum initial span of angles can be determined if the range of wave-speed variation is known approximately. Then, we use the ray equations to trace the rays at each of these angles through the medium to the vicinity of the receiver of interest. Normally none of the initial angles turns out to be the correct one (*i.e.*, the one that produces a ray that hits the receiver), but often the receiver is bracketed by two of these rays. Then, by interpolation, we can find as accurate an approximation as we like: *i.e.*, choose a new set of angles between the pair that brackets the receiver, trace the rays for these angles, keep the two closest that bracket the receiver, and continue this process until some closeness objective has been achieved.

Shooting methods are very accurate, but also relatively expensive. We may have to shoot many rays to achieve the desired degree of accuracy. Furthermore, there can be pathological cases arising in inversion and tomography where it is difficult or impossible to trace a ray from the the source to receiver through the current best estimate of the slowness model. Such problems are most likely to occur for models containing regions with high contrasts. Then, there can exist shadow zones behind slow regions, where ray amplitude is small for first arrivals. Such problems can also arise due to poor choice of model parametrization. Shooting methods should normally be used with smooth models based on bilinear interpolation between grid points, or spline function approximations. If the desired model uses cells of constant slowness, shooting methods are not recommended.

Problems

Problem 5.3.1 *Verify (5.11).*

Problem 5.3.2 *Derive Snell's law (5.2) for the change in ray angle at a plane interface from the ray equation (5.11).*

Problem 5.3.3 *Can the ray equation be derived from Snell's law?*

Problem 5.3.4 *Consider a horizontally stratified medium with a sequence of layers having uniform slownesses s_1, s_2, s_3, ... Use Snell's law to show that a ray having angle θ_1 to the vertical in the first layer will have an associated invariant (called the ray parameter)*

$$\boxed{p \;=\; s_i \sin\theta_i} \tag{5.17}$$

in every layer i whose slowness satisfies $s_i > s_1 \sin\theta_1$. If the ray encounters a layer (say the nth layer) whose slowness satisfies $s_n \leq s_1 \sin\theta_1$, then what happens? Show that the constancy of the ray parameter is a direct consequence of (5.16).

5.4 The Eikonal Equation

Consider the wave equation for a field $\psi(\mathbf{x}, t)$ in a medium with slowness $s(\mathbf{x})$:

$$\nabla^2\psi = s^2(\mathbf{x})\frac{\partial^2\psi}{\partial t^2}. \tag{5.18}$$

Let us assume

$$\psi(\mathbf{x}, t) = e^{i\omega[\phi(\mathbf{x})-t]} = e^{-\omega\Im\phi(\mathbf{x})}e^{i\omega[\Re\phi(\mathbf{x})-t]}, \tag{5.19}$$

where $\phi(\mathbf{x}) = \Re\phi(\mathbf{x}) + i\Im\phi(\mathbf{x})$ is a complex phase. The imaginary part $\Im\phi$ determines the amplitude of ψ. Substituting into the wave equation, we get

$$\left[i\omega\nabla^2\phi - \omega^2\nabla\phi\cdot\nabla\phi + \omega^2 s^2(\mathbf{x})\right]\psi = 0. \tag{5.20}$$

In the limit $\omega \to \infty$, $\phi \to \Re\phi$, since (5.20) implies that

$$\nabla\Re\phi\cdot\nabla\Re\phi - \nabla\Im\phi\cdot\nabla\Im\phi = s^2(\mathbf{x}) \tag{5.21}$$

and

$$\nabla\Re\phi\cdot\nabla\Im\phi = 0, \tag{5.22}$$

and the wave equation reduces to the *eikonal*[2] *equation*

$$\boxed{|\nabla\phi| \quad = \quad s(\mathbf{x}).} \tag{5.23}$$

5.5 Vidale's Method

The method of Vidale (1988) uses a finite difference scheme to compute the traveltimes of waves in an arbitrary medium. The slowness of the medium is represented on the nodes of a rectilinear grid with bilinear (for 2-D media) interpolation assumed between nodes. The method approximates the wave field which propagates through a given element as a plane wave. This approximation is valid for the far field. (A different approach is used for the near field, but we will not cover this here.)

5.5.1 Algebraic derivation

Figure 5.3 shows one element of the grid. We number the nodes of the element in a counterclockwise manner, starting with the lower left node. Without loss of generality, we let the plane wave begin at node 0 with traveltime t_0, assumed known. The traveltime to the other nodes—t_1, t_2 and t_3—will then be greater than t_0 by an amount which depends

[2] The term *eikonal* (from the Greek $\varepsilon\iota\kappa\tilde{\omega}\nu$ meaning *icon* or *image*) was introduced by Bruns [1895].

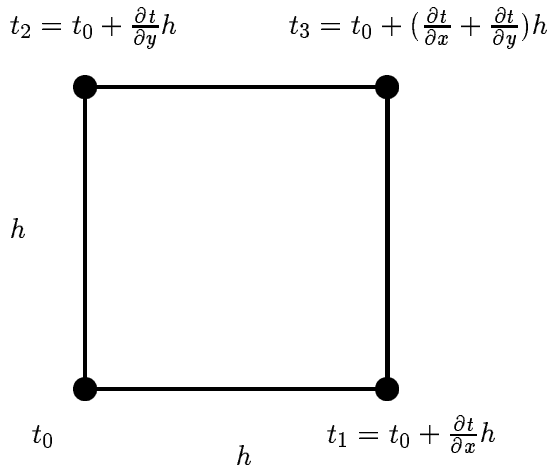

Figure 5.3: Diagram of a grid element used in Vidale's method.

on the direction of propagation and the grid element size h. In general we can write the Taylor series expansion

$$t_1 = t_0 + \frac{\partial t}{\partial x} h, \tag{5.24}$$

$$t_2 = t_0 + \frac{\partial t}{\partial y} h, \tag{5.25}$$

$$t_3 = t_0 + \left(\frac{\partial t}{\partial x} + \frac{\partial t}{\partial y} \right) h, \tag{5.26}$$

valid to first order in h. We can solve these equations for the gradient of t, obtaining

$$2h \frac{\partial t}{\partial x} = t_3 + t_1 - t_2 - t_0, \tag{5.27}$$

$$2h \frac{\partial t}{\partial y} = t_3 + t_2 - t_1 - t_0. \tag{5.28}$$

The eikonal equation implies that $|\nabla t|^2 = s^2(\mathbf{x})$. If we substitute from (5.27) and (5.28) for ∇t and an element average value of s, we get

$$(t_3 + t_1 - t_2 - t_0)^2 + (t_3 + t_2 - t_1 - t_0)^2 = 4\bar{s}^2 h^2, \tag{5.29}$$

where

$$\bar{s} = \frac{1}{4}(s_0 + s_1 + s_2 + s_3). \tag{5.30}$$

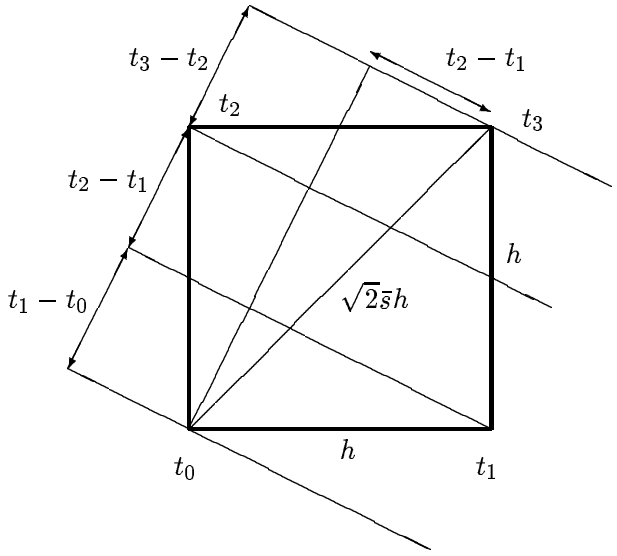

Figure 5.4: Geometry of plane wavefront incident on a grid element.

From (5.29), we find that the cross terms cancel so

$$(t_3 - t_0)^2 + (t_1 - t_2)^2 = 2\bar{s}^2 h^2. \tag{5.31}$$

Solving for t_3, we get *Vidale's formula*:

$$t_3 = t_0 + \sqrt{2\bar{s}^2 h^2 - (t_1 - t_2)^2}. \tag{5.32}$$

We can verify (5.32) for two limiting cases. First, for a wave traveling in the $+x$ direction, we must have $t_0 = t_2$ and, assuming s is constant, $t_1 = t_0 + \bar{s}h$. Substituting these into (5.32) then yields $t_3 = t_0 + \bar{s}h$, which is intuitively the correct answer. Similarly, Vidale's formula implies $t_3 = t_0 + \sqrt{2}\bar{s}h$ for a wave travel at 45 degrees to x, i.e., when $t_1 = t_2$.

5.5.2 Geometric derivation

We can gain more insight into the significance of Vidale's method by deriving the result another way. Now consider Fig. 5.4. We assume that to a first approximation it is satisfactory to treat the slowness in the cell as constant. The constant we choose is the average of the four grid slownesses at the corners of the cell $\bar{s} = 0.25(s_1 + s_2 + s_3 + s_4)$. If the planewave impinges on the cell from the lower left, making angle θ with the x-axis, then the simple geometrical construction in the figure shows that the following identities must hold:

$$t_1 - t_0 = \bar{s}h\cos\theta, \tag{5.33}$$

$$t_3 - t_2 = \bar{s}h\cos\theta, \tag{5.34}$$

$$t_2 - t_0 = \bar{s}h\sin\theta, \tag{5.35}$$

$$t_3 - t_1 = \bar{s}h\sin\theta. \tag{5.36}$$

We see directly from Fig. 5.4 that the right triangle whose hypotenuse is the diagonal of the cell and whose longest side is proportional to the time difference $t_3 - t_0$ has its short side proportional to $t_2 - t_1$. The Pythagorean theorem then tells us that

$$(t_3 - t_0)^2 + (t_2 - t_1)^2 = 2\bar{s}^2h^2, \tag{5.37}$$

in agreement with (5.31) and (5.32). Alternatively, we see that (5.33)–(5.36) show

$$(t_3 - t_0)^2 + (t_2 - t_1)^2 = \bar{s}^2h^2(\cos\theta + \sin\theta)^2 + \bar{s}^2h^2(\sin\theta - \cos\theta)^2 = 2\bar{s}^2h^2. \tag{5.38}$$

From our examination of the geometry for planewaves, we get a bonus. Now we can also find a simple estimate of the angle θ if we know the traveltimes. Clearly,

$$\tan\theta = \frac{t_2 - t_0}{t_1 - t_0} = \frac{t_3 - t_1}{t_3 - t_2} \tag{5.39}$$

follows from (5.33)–(5.36). It also follows from (5.27) and (5.28) that

$$\tan\theta = \frac{\partial t/\partial y}{\partial t/\partial x} = \frac{t_3 + t_2 - t_1 - t_0}{t_3 + t_1 - t_2 - t_0}, \tag{5.40}$$

a result that we may also infer from (5.33)–(5.36). Thus, it is possible to determine the angle θ to first order just by knowing the traveltimes at the corners of the cell. This fact suggests several alternatives for adding ray tracing to Vidale's finite difference traveltime computation, but we will not pursue that subject here.

Finally, note that (5.33)-(5.36) show that

$$t_3 = t_2 + t_1 - t_0. \tag{5.41}$$

Why is this *not* a useful identity for computing the traveltimes?

5.6 Bending Methods

Although in principle they can be, in practice bending methods are generally not as systematic or as accurate as shooting methods. However, they are also much less prone to convergence failures in the presence of pathological models with high relative contrasts (which can result in shadow zones occurring behind very slow regions). Bending methods start with some connected path between the source and receiver (generally a straight line for borehole-to-borehole tomography) and then use some method to reshape or bend that path to reduce and (we hope) minimize the overall traveltime along the path. Bending methods are conceptually based on Fermat's principle of least time; the minimization over paths in (1.2) is being performed now essentially using trial and error. This method is just as legitimate as the others discussed previously and can be just as accurate if the search routine is

sufficiently sophisticated. Also, bending methods are the only ones that I recommend using when the model is composed of cells of constant slowness. Other methods such as shooting take the cell boundaries in these models too seriously — trying to satisfy Snell's law exactly at these artificial boundaries while the approximate satisfaction of Snell's law achieved by the bending method using Fermat's principle is more consistent with the approximation to the physics embodied in the model.

5.6.1 The method of Prothero, Taylor, and Eickemeyer

We summarize the bending method of Prothero, Taylor, and Eickemeyer (1988) for the case of 2-D ray paths.

Let (x_S, y_S) and (x_R, y_R) be the given endpoints of the ray. We seek the least time path between the two points, which we can describe with the function $y(x)$ or $x(y)$. [It is assumed that one of these functions is single valued.] Let us use $y(x)$ and, with no loss of generality, we take $x_S = 0$, $x_R = L$.

In ray bending, we begin with an initial ray $y_0(x)$ and seek a perturbation $\delta y(x)$ to the initial ray such that the traveltime along the perturbed ray is reduced. Typically the initial ray is taken to be a straight line:

$$y_0(x) = y_S(1 - \frac{x}{L}) + y_R\frac{x}{L}. \tag{5.42}$$

The perturbed ray is taken to be a harmonic series of the form

$$\delta y(x) = \sum_{k=1}^{K} a_k \sin\frac{k\pi x}{L}. \tag{5.43}$$

The order of the series is usually kept small (e.g., $K = 2$). Note that only sine, and not cosine, terms are used so that the endpoints of the ray remain unperturbed.

In terms of the $y(x)$, the traveltime is given by

$$t = \int_0^L s(x, y(x))\sqrt{1 + (dy/dx)^2}\, dx. \tag{5.44}$$

Prothero, Taylor, and Eickemeyer (1988) use the Nelder-Mead search procedure [Nelder and Mead, 1965; Press, Flannery, Teukolsky, and Vetterling, 1988] to find coefficients a_k such that the traveltime is reduced. The Nelder-Mead approach may be used in any number of dimensions to seek the minimum of a complicated function, especially when local gradients of the function are difficult or expensive to compute. The main idea is to perform a sequence of operations on an n-dimensional simplex, so that the vertices of the simplex converge on the point where the function is minimum. In 2-D, the simplex is a triangle. The complicated function to be minimized in our problem is the traveltime functional. Using this approach, the traveltimes associated with three choices of the ordered pairs (a_1, a_2) are compared—for example, the origin $(0, 0)$ and two other points in the a_1a_2-plane. The point with the largest traveltime is then replaced with a new point found as the mirror reflection of the point about a line passing through the other two points.

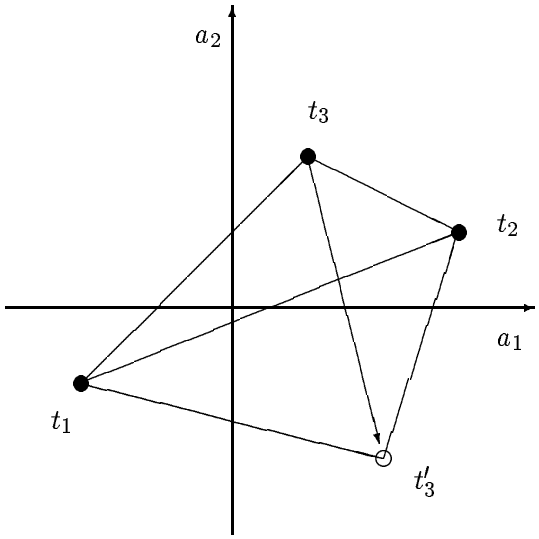

Figure 5.5: Illustration of the Nelder-Mead method.

Figure 5.5 illustrates the method. Starting with three points whose corresponding traveltimes are respectively $t_1 < t_2 < t_3$, the algorithm seeks to replace the point with the largest traveltime by a smaller traveltime t_3'. The figure shows the first attempt in such a process, which is usually reflection of the triangle across the line determined by the other two vertices of the triangle. If the traveltime associated with this point satisfies $t_3' < t_2$, then this point becomes a point of the new triangle. If $t_3' > t_2$, then other moves are made such as checking values between the original vertex and the reflected vertex or expansion/contraction of the triangle. When an improved (smaller traveltime) vertex is found, the vertices are relabelled and the process starts over for the new triangle. If no improvement (or improvement less than some preset threshold) is attained or some fixed number of iterations is exceeded, the process terminates for this ray path.

5.6.2 Getting started

One potential pitfall of this method occurs when attempting to choose a set of vertices for the starting triangle that avoids biasing the final results. Bias in this context means a tendency to choose rays that bow away from the straight path in the same direction. I recommend always choosing the origin $(a_1, a_2) = (0, 0)$ as one of the initial vertices, since this choice corresponds to a straight ray path and is clearly unbiased by definition. The straight path may be a good approximation to the true path whenever the wave speed constrasts in the model are low. Then, how should the other two vertices be chosen?

One rather obvious pairing can be excluded immediately: Suppose that we choose the point $(a_1, a_2) = (\alpha, \beta)$. Then the mirror image of the path across the source/receiver line is given by the point $(a_1, a_2) = (-\alpha, -\beta)$. However, rather than determining a triangle, these three points $(-\alpha, -\beta), (0,0), (\alpha, \beta)$ form a straight line in the $a_1 a_2$-plane. Thus, although pairing (α, β) with $(-\alpha, -\beta)$ is desirable from the point of view of minimizing bias, this pairing produces an undesirable degenerate version of the triangle needed in the Nelder-Mead algorithm. Therefore, we should exclude this possibility.

In general, we should expect the ray bending effect to be dominated by the coefficient a_1. Thus, although there clearly may be exceptions, we generally expect $|a_1| > |a_2|$ and very often $|a_1| >> |a_2|$. So we try to minimize the bias in the initial choice of vertices by pairing (α, β) with $(-\alpha, \beta)$, where $|\beta|$ is about an order of magnitude smaller than $|\alpha|$. This choice of pairing eliminates the major source of bias in the initial simplex while still producing a usable triangle for the Nelder-Mead algorithm. The precise value to be used for α depends on the expected range of variation (or contrast) in the wave speed in the region being imaged. In fact, the initial choice of α for this approach is closely related to the optimum choice of the maximum initial span of angles needed to start the shooting methods described earlier.

5.7 Comparison

On average, the method of Prothero *et al.* (1988) has been found to be as fast and as accurate as Vidale's method when 100 times fewer cells are used than in Vidale's modelization. So the bending method is considerably more accurate on a coarser grid, but also corresponding slower to compute. Vidale's method is not as accurate as the bending method for regions that are very slow compared to the background, due to limitations it has in or near shadow zones. The bending method is not quite as accurate as Vidale's method for regions of high wave speed relative to background and comparable computing time, apparently due to limitations of the ray parameterization embodied in (5.43). The hybrid approach of using the best (smallest) traveltimes found by either method as the "true" traveltime has been tested and gives better results than either method alone.